

## Extreme Ultraviolet Frequency Comb Metrology

Dominik Z. Kandula, Christoph Gohle,\* Tjeerd J. Pinkert, Wim Ubachs, and Kjeld S. E. Eikema<sup>†</sup>

*Institute for Lasers, Life and Biophotonics Amsterdam, VU University, De Boelelaan 1081, 1081HV Amsterdam, The Netherlands*

(Received 28 April 2010; revised manuscript received 24 June 2010; published 2 August 2010)

The remarkable precision of frequency-comb (FC) lasers is transferred to the extreme ultraviolet (XUV, wavelengths shorter than 100 nm), a frequency region previously not accessible to these devices. A frequency comb at XUV wavelengths near 51 nm is generated by amplification and coherent up-conversion of a pair of pulses originating from a near-infrared femtosecond FC laser. The phase coherence of the source in the XUV is demonstrated using helium atoms as a ruler and phase detector. Signals in the form of stable Ramsey-like fringes with high contrast are observed when the FC laser is scanned over  $P$  states of helium, from which the absolute transition frequency in the XUV can be extracted. This procedure yields a  $^4\text{He}$  ionization energy at  $h \times 5\,945\,204\,212(6)$  MHz, improved by nearly an order of magnitude in accuracy, thus challenging QED calculations of this two-electron system.

DOI: 10.1103/PhysRevLett.105.063001

PACS numbers: 32.10.Hq, 42.62.Eh, 42.65.Ky

Mode-locked frequency-comb (FC) lasers [1,2] have revolutionized the field of precision laser spectroscopy. Optical atomic clocks using frequency combs are about to redefine the fundamental standard of frequency and time [3]. FC lasers have also vastly contributed to attosecond science by providing a way to synthesize electric fields at optical frequencies [4], made long distance absolute length measurements possible [5], and have recently been employed to produce ultracold molecules [6]. FC based precision spectroscopy on simple atomic systems has provided one of the most stringent tests of bound state quantum electrodynamics (QED) as well as upper bounds on the drift of fundamental constants [7]. Extending these methods into the extreme ultraviolet (XUV, wavelengths below 100 nm) spectral region is highly desirable since this would, for example, allow novel precision QED tests [8].

Currently the wavelength range below 120 nm is essentially inaccessible to precision frequency metrology applications due to a lack of power of single frequency lasers and media for frequency up-conversion. Spectroscopic studies on neutral helium using amplified nanosecond laser pulses [9,10] are notoriously plagued by frequency chirping during amplification and harmonic conversion which limits the accuracy. These kind of transient effects can be avoided if a continuous train of high power laser pulses (produced by a FC) can be coherently up-converted. This would transfer the FC modes, at frequencies  $f_n = f_{\text{CEO}} + n f_{\text{rep}}$ , where  $f_{\text{CEO}}$  is the carrier-envelope offset frequency,  $f_{\text{rep}}$  is the repetition frequency of the pulses, and  $n$  an integer mode number, to the XUV. Similar to what was shown in the visible [11,12], the up-converted pulse train could be used to directly excite a transition, with each of the up-converted modes acting like a single frequency laser.

By amplification of a few pulses from the train, and producing low harmonics in crystals and gasses, sufficient coherence has been demonstrated down to 125 nm to perform spectroscopic experiments [13,14]. To reach

wavelengths below 120 nm in the extreme ultraviolet or even x rays, high harmonic generation (HHG) has to be employed requiring nonlinear interaction at much higher intensities in the nonperturbative regime [15]. That HHG can be phase coherent to some degree is known [15–17], and recently XUV light has been generated based on up-conversion of all pulses of a comb laser at full repetition rate [18–21]. However, no comb structure in the harmonics has been demonstrated in the XUV, nor had these sources enough power to perform a spectroscopic experiment.

In this Letter we show that these limitations can be overcome, leading to the first absolute frequency measurement in the XUV. Instead of converting a continuous train of FC pulses, we amplify a pair of subsequent pulses from an IR frequency-comb laser with a double-pulse parametric amplifier (OPA) [22] to the milli-joule level. These pulses with time separation  $T = 1/f_{\text{rep}}$  can be easily up-converted into the XUV with high efficiency using HHG in a dilute gaseous medium, and used to directly excite a transition in atoms or molecules [see Figs. 1(a) and 1(c)]. This form of excitation with two pulses resembles an optical (XUV) variant of Ramsey spectroscopy [13,23]. Excitation of an isolated (atomic or molecular) resonance with two (nearly) identical pulses produces a signal which is cosine-modulated according to  $\cos(2\pi(f_{\text{tr}}T) - \Delta\phi(f_{\text{tr}}))$ , where  $f_{\text{tr}}$  is the transition frequency and  $\Delta\phi(f_{\text{tr}})$  is the spectral phase difference between the two pulses at the transition frequency. Ideally, this spectral phase difference is just  $\Delta\phi(f) = q\Delta\phi_{\text{CE}} = 2q\pi f_{\text{CEO}}/f_{\text{rep}}$ , where  $q$  is the harmonic order under consideration and  $\Delta\phi_{\text{CE}}$  the carrier-envelope offset phase slip between subsequent pulses of the FC. In this case the cosine-modulated spectroscopy signal has a maximum whenever one of the modes of an up-converted frequency comb would be resonant. This statement remains true even if the amplification and harmonic up-conversion significantly distorts the electric field of the individual pulses as long as these distortions are common mode for each of

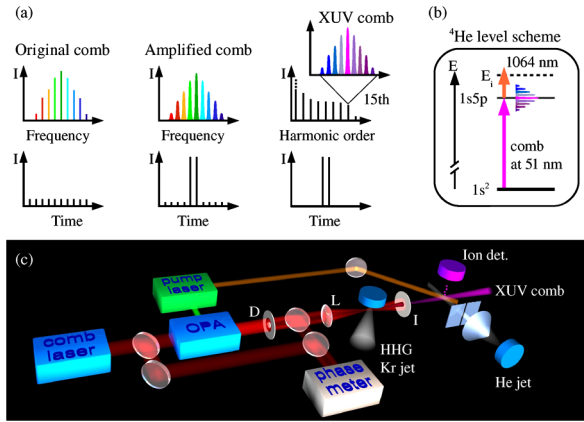


FIG. 1 (color online). (a) Spectral and temporal structure of the generated light (left to right): FC of the continuous coherent pulse train from the FC laser, the cosine-modulated spectrum of a pair of amplified pulses, and odd harmonics of the amplified FC laser pulses each containing a cosine-modulated XUV comb corresponding to the XUV pulse pair. (b) Simplified  $^4\text{He}$  level scheme, XUV comb excitation at 51.5 nm from the  $1s^2$  ground state to the  $1s5p$  excited state and state-selective ionization by a pulse at 1064 nm. (c) Schematic of the experimental setup. *D*: beam mask, *L*: focusing lens,  $f = 50$  cm, *I*: iris to separate XUV from IR. The pump laser provides both the 532 nm for pumping the OPA as well as 1064 nm for ionization of helium.

them. Distortions that are not common mode need to be monitored and corrected for, in this experiment at a level of  $<1/200$ th of the fundamental IR field period. The frequency accuracy of the method is not fundamentally limited by the accuracy of this correction since an error  $\delta$  in  $\Delta\phi(f)$  translates into a frequency error  $\Delta f = \delta/(2\pi T)$ . Therefore the error can be made arbitrarily small by increasing the time separation  $T$  between the pulses, provided the coherence time of the excited state allows this.

Phase coherent pulses near 773 nm are obtained from a Ti:sapphire frequency comb (repetition rate  $f_{\text{rep}}$  between 100 and 185 MHz), which is linked to a GPS-controlled rubidium clock (Stanford research PRS10) to reach a frequency stability on the order of  $10^{-11}$  after a few seconds of averaging. A bandwidth of 6 nm (rectangular spectrum, leading to  $\approx 300$  fs pulses after compression) is selected from the FC laser so that after up-conversion to the XUV only one state in helium is excited at a time. A noncollinear parametric double-pulse amplifier [22] is used to amplify two subsequent FC pulses (5.5–10 ns apart) at a repetition rate of 28 Hz. Parametric amplification intrinsically has small transient effects [24] so that differential pulse distortions are kept to a minimum. They are monitored using spectral interferometry with the unaltered FC pulses as a reference [22]. Wave front deformations in the amplified beam are reduced by spatial filtering. The differential phase shift from the amplifier and subsequent optics has a magnitude of typically 100 mrad in the IR. Spatial and spectral variations are at most 20–30 mrad. The IR beam is converted to a doughnut mode by a small disk mask

(1.9 mm diameter compared to a beam diameter of 6 mm) to separate the XUV from the IR after HHG. The remaining 1–2 mJ per pulse is focused in a pulsed krypton gas jet to  $<5 \times 10^{13}$  W/cm $^2$  for HHG. This combination is chosen such that the 15th harmonic is exactly at the cutoff, so that higher harmonics are strongly suppressed. An iris of 0.8 mm diameter placed at 40 cm distance after the focus allows the XUV to pass without significant losses or beam distortion, but blocks the IR with a contrast ratio of 27:1. For the 15th harmonic at 51.5 nm generated in the krypton gas we estimate a yield of about  $1 \times 10^8$  photons per pulse.

The resulting XUV beam intersects a low divergence beam of helium atoms at perpendicular angle to avoid a Doppler shift. This beam is generated in a supersonic pulsed expansion (backing pressure 3 bar) using a differential pumping stage containing two skimmers which limit the beam divergence to roughly 3–4 mrad. This is similar to the divergence of the XUV beam ( $<2$  mrad). The second skimmer position can be adjusted to set the XUV-He beam angle. To investigate Doppler effects, helium can be seeded in heavier noble gases (partial pressure ratio 1:5). Pure helium results in a velocity of 2000(315) m/s, while seeding in neon and argon leads to a helium velocity of 830(200) and 500(250) m/s, respectively.

Helium atoms in the atomic beam are excited by the double pulse from the ground state into upper states which have spectral overlap with the HHG radiation [Fig. 1(b)]. After the double-pulse has passed, the excited state population is determined by state-selective ionization of the helium atoms using 60 ps, 1064 nm pulses from the OPA pump laser, followed by mass selective detection of the resulting ions in a time of flight spectrometer. Higher harmonics than the 15th are at least 10 times weaker, and produce a constant background signal of only 15% of the relevant spectroscopic signal due to direct ionization. The 13th and lower order harmonics are not resonant with any transition from the ground state of helium.

Figure 2 shows a typical recording of the  $^4\text{He}$  ion signal, where the laser center frequency is tuned to the  $1s^2$   $^1S_0$ – $1s5p$   $^1P_1$  transition and the repetition frequency of the frequency comb is scanned. Recording such a trace takes about 20000 laser shots, corresponding to ten minutes of continuous data taking. After correction for the measured IR phase shifts and XUV intensity, the data points are binned into 20 groups per Ramsey period. During a recording the pulse delay  $T$  is changed in steps of typically less than 1 attosecond every 28 laser shots, with a total change over a scan of less than 1 femtosecond.

By fitting the phase of the expected cosine function to this signal, we determine the transition frequency up to an integer multiple of the laser repetition frequency  $f_{\text{rep}}$ . The statistical error in the fit of a single recording is typically 1/50th of a modulation period. Depending on the repetition rate it amounts to a uncertainty of 2–3 MHz in the

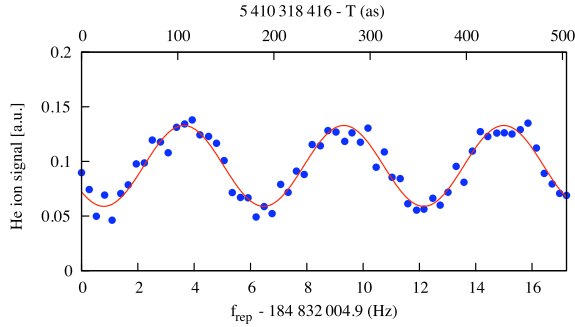


FIG. 2 (color online). Measured excitation probability (blue circles) of helium at 51.5 nm on the  $1s^2\ ^1S_0 - 1s5p\ ^1P_1$  transition, normalized by the XUV pulse energy, as a function of the repetition rate  $f_{\text{rep}}$  of the frequency-comb laser. In this example  $f_{\text{CEO}}$  is locked at 46.21 MHz, and a 1:5 He:Ne mixture is used for the atomic beam. The red line is a fit to the data.

observed transition frequency, which is unprecedented in the XUV spectral region. Such scans are repeated many times to assess systematic effects. The dominant systematic shifts are Doppler shift and a differential phase shift of the XUV pulses due to changing levels of ionization of the HHG medium. The former is minimized by setting the XUV-helium beam angle perpendicular. It is evaluated by varying the speed of the helium beam and extrapolating the observed transition frequency to zero velocity. The ionization shift is found by varying the HHG medium density (assuming the ionized fraction remains constant) and extrapolating to zero density. The statistical error in the latter extrapolation dominates the final statistical error. Systematic errors in Doppler shift and ionization shift originate in the uncertainty of the helium velocity and ionization dynamics in the HHG medium, respectively. Other effects that are taken into account include recoil shifts, refractive index changes (Kerr effect) in the focusing lens for HHG and the entrance window to the vacuum setup, ac and dc-Stark effect and Zeeman shift. A summary of the error budget can be found in Table I. Most recordings were made on the  $1s^2\ ^1S_0 - 1s5p\ ^1P_1$  transition at 51.5 nm. As a cross check also a series was measured on the  $1s^2\ ^1S_0 - 1s4p\ ^1P_1$  transition at 52.2 nm. The  $^4\text{He}$  ionization potential (up to an integer multiple of  $f_{\text{rep}}$ ) is derived from

TABLE I. The major contributions to the error budget of the ionization potential expressed as frequencies.

Statistical error	3.7 MHz
Ionization shift	4.9 MHz
Doppler shift	500 kHz
dc-Stark shift	<1 kHz
Signal from other levels	<30 kHz
Zeeman shift	<7 kHz
Total	6 MHz

these measurements by adding the excited state ionization energy of the  $4p$  and  $5p$ . The energy of these states is known with an accuracy better than 20 kHz based on theoretical calculations [25].

To remove the ambiguity due to the periodic comb spectrum, we repeated this procedure for several repetition frequencies within the range of 100 MHz and 185 MHz. The correct “mode number” is found by plotting the possible ionization energies of the helium ground state against  $f_{\text{rep}}$  as shown in Fig. 3. A clear coincidence between the results for different repetition rates can be seen, leading to a new ground state ionization energy for  $^4\text{He}$  of 5 945 204 212(6) MHz by taking a weighted average over all measured frequencies at the coincidence location. This is in agreement with recent theoretical predictions of 5 945 204 174(36) MHz [26] and 5 945 204 175(36) MHz [27] within the combined uncertainty of theory and experiment. Compared to previous experiments employing single nanosecond duration laser pulses, we find good agreement with the value of 5 945 204 215(45) MHz [9] (using the most recent  $2p$  state ionization energy [26], and corrected for a 14.6 MHz recoil shift that was previously not taken into account). However, there is a difference of nearly  $3\sigma$  compared to a competing result [10].

From the observed signal contrast (defined as the modulation amplitude divided by the average signal level) we can infer the temporal coherence of the HHG process. The contrast depends on several parameters: the upper state lifetime (natural linewidth), the time between the pulses, a difference in XUV pulse energy of the two pulses, the frequency stability of the interference pattern, Doppler broadening of the transition, and the previously mentioned constant background from direct ionization due to the 17th and higher harmonics. The Doppler broadening is dominated by the effective atomic beam opening angle and the

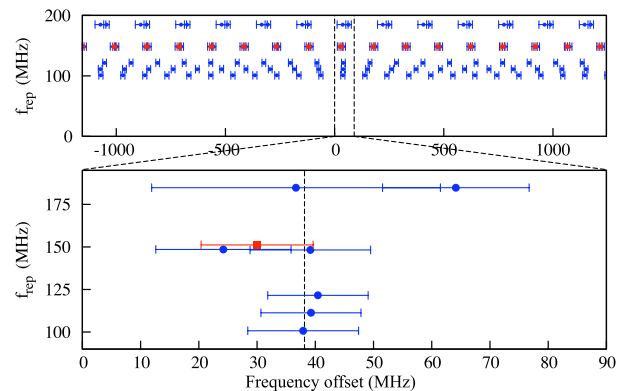


FIG. 3 (color online). (top)  $^4\text{He}$  ground state ionization energy  $\pm n \times f_{\text{rep}}$  based on the  $1s^2\ ^1S_0 - 1s5p\ ^1P_1$  (blue circles) and the  $1s^2\ ^1S_0 - 1s4p\ ^1P_1$  transition (red squares). (bottom) Zoom at the coincidence point for all repetition frequencies. The vertical line at +38(6) MHz represents the weighted mean. All values are relative to the theoretical value of 5 945 204 174 MHz [26]. (square point slightly shifted up for visibility).

radial velocity of the beam. All these effects lead to a varying contrast depending on the helium velocity  $v$  and comb repetition frequency. For a high repetition rate ( $f_{\text{rep}} = 185$  MHz) and low  $v$  (helium seeded in argon), we find a fringe contrast of 55%, while on the other hand for  $f_{\text{rep}} = 100$  MHz and a pure helium beam (large  $v$ ) the contrast is below 5%. From these observed variations and a straight forward model for the visibility as a function of  $f_{\text{rep}}$  and atomic beam velocity, we estimate a phase jitter of 0.38(6) cycles in the XUV. To a large part this can be attributed to the timing noise of the driving IR pulses (0.014 cycles rms), leading to an estimated jitter in the XUV of 0.21 cycles. This noise in turn comes mostly from the radio frequency  $f_{\text{rep}}$  lock of the frequency-comb laser, which can be improved by locking the FC to an optical reference resonator.

In conclusion, we have demonstrated frequency-comb generation in the XUV and performed the first absolute frequency determination in this spectral region. Based on the contrast of the helium excitation signal we find that the excess phase noise in the HHG process used to generate the XUV comb is at most 0.3 optical cycles in the XUV. This means that the timing of the generated electric field of the XUV waveform of individual pulses is stable within less than 50 as, which is an important benchmark for both spectroscopy applications as well as ultrafast physics. The new value of the  $^4\text{He}$  ionization potential is in good agreement with theory [26,27] and already almost an order of magnitude more accurate than the best previous results using single nanosecond laser pulses [9,10]. Moreover, the accuracy of our method can readily be improved by orders of magnitude by increasing the time delay between the two pulses. One could, for example, perform high resolution spectroscopy on the  $1s - 2s$  two photon transition of hydrogenlike helium ions at 60 nm, which is very promising to perform QED tests beyond what has been possible so far in atomic hydrogen [8,28]. The results show that as long as the carrier phase noise is kept low enough not to destroy the mode structure, comb generation should be extendable to the soft x-ray region. This may allow applications such as coherent XUV and x-ray imaging, precision QED tests of (highly) charged ions, to perhaps ultimately x-ray nuclear clocks.

This work was supported by the FOM through its IPP-program “Metrology with Frequency Comb Lasers,” by the NWO, by the EU via the “Atlas” network, and by the Humboldt Foundation.

\*Present address: Ludwig-Maximilians-Universität München, Schellingstrasse 4, 80799 München, Germany.

†KSE.Eikema@few.vu.nl

- [1] R. Holzwarth, T. Udem, T. W. Hänsch, J. C. Knight, W. J. Wadsworth, and P. S. J. Russell, *Phys. Rev. Lett.* **85**, 2264 (2000).
- [2] S. A. Diddams, D. J. Jones, J. Ye, S. T. Cundiff, J. L. Hall, J. K. Ranka, R. S. Windeler, R. Holzwarth, T. Udem, and T. W. Hänsch, *Phys. Rev. Lett.* **84**, 5102 (2000).
- [3] T. Rosenband *et al.*, *Science* **319**, 1808 (2008).
- [4] A. Baltuška *et al.*, *Nature (London)* **421**, 611 (2003).
- [5] I. Coddington, W. C. Swann, L. Nenadovic, and N. R. Newbury, *Nat. Photon.* **3**, 351 (2009).
- [6] K. K. Ni, S. Ospelkaus, M. H. G. de Miranda, A. Pe'er, B. Neyenhuis, J. J. Zirbel, S. Kotochigova, P. S. Julienne, D. S. Jin, and J. Ye, *Science* **322**, 231 (2008).
- [7] T. W. Hänsch, J. Alnis, P. Fendel, M. Fischer, C. Gohle, M. Herrmann, R. Holzwarth, N. Kolachevsky, T. Udem, and M. Zimmermann, *Phil. Trans. R. Soc. A* **363**, 2155 (2005).
- [8] M. Herrmann *et al.*, *Phys. Rev. A* **79**, 052505 (2009).
- [9] K. S. E. Eikema, W. Ubachs, W. Vassen, and W. Hogervorst, *Phys. Rev. A* **55**, 1866 (1997).
- [10] S. D. Bergeson *et al.*, *Phys. Rev. Lett.* **80**, 3475 (1998).
- [11] A. Marian, M. C. Stowe, D. Felinto, and J. Ye, *Phys. Rev. Lett.* **95**, 023001 (2005).
- [12] P. Fendel, S. D. Bergeson, T. Udem, and T. W. Hänsch, *Opt. Lett.* **32**, 701 (2007).
- [13] S. Witte, R. T. Zinkstok, W. Ubachs, W. Hogervorst, and K. S. E. Eikema, *Science* **307**, 400 (2005).
- [14] R. T. Zinkstok, S. Witte, W. Ubachs, W. Hogervorst, and K. S. E. Eikema, *Phys. Rev. A* **73**, 061801 (2006).
- [15] M. Lewenstein, P. Balcou, M. Y. Ivanov, A. L'Huillier, and P. B. Corkum, *Phys. Rev. A* **49**, 2117 (1994).
- [16] R. Zerne, C. Altucci, M. Bellini, M. B. Gaarde, T. W. Hänsch, A. L'Huillier, C. Lyngå, and C. G. Wahlström, *Phys. Rev. Lett.* **79**, 1006 (1997).
- [17] S. Cavalieri, R. Eramo, M. Materazzi, C. Corsi, and M. Bellini, *Phys. Rev. Lett.* **89**, 133002 (2002).
- [18] R. J. Jones, K. D. Moll, M. J. Thorpe, and J. Ye, *Phys. Rev. Lett.* **94**, 193201 (2005).
- [19] C. Gohle, T. Udem, M. Herrmann, J. Rauschenberger, R. Holzwarth, H. A. Schuessler, F. Krausz, and T. W. Hänsch, *Nature (London)* **436**, 234 (2005).
- [20] A. Ozawa *et al.*, *Phys. Rev. Lett.* **100**, 253901 (2008).
- [21] D. C. Yost, T. R. Schibli, J. Ye, J. L. Tate, J. Hostetter, M. B. Gaarde, and K. J. Schafer, *Nature Phys.* **5**, 815 (2009).
- [22] D. Z. Kandula, A. Renault, C. Gohle, A. L. Wolf, S. Witte, W. Hogervorst, W. Ubachs, and K. S. E. Eikema, *Opt. Express* **16**, 7071 (2008).
- [23] N. F. Ramsey, *Phys. Rev.* **76**, 996 (1949).
- [24] A. Renault, D. Z. Kandula, S. Witte, A. L. Wolf, R. T. Zinkstok, W. Hogervorst, and K. S. E. Eikema, *Opt. Lett.* **32**, 2363 (2007).
- [25] D. C. Morton, Q. X. Wu, and G. W. F. Drake, *Can. J. Phys.* **84**, 83 (2006).
- [26] V. A. Yerokhin and K. Pachucki, *Phys. Rev. A* **81**, 022507 (2010).
- [27] G. W. F. Drake and Z. C. Yan, *Can. J. Phys.* **86**, 45 (2008).
- [28] M. Fischer *et al.*, *Phys. Rev. Lett.* **92**, 230802 (2004).